doi.org/10.1002/cbdv.202300611 Research Article CHEMISTRY & BIODIVERSITY

www.cb.wiley.com

Synthesis and Characterization of Novel 1,3-Diaryltriazene-Substituted Sulfaguanidine Derivatives as Selective Carbonic Anhydrase Inhibitors: Biological Evaluation, *in Silico* ADME/T and Molecular Docking Study

Suleyman Akocak,*[a] Nebih Lolak,[a] Hatice Esra Duran,[b] Mesut Işık,*[c] Cüneyt Türkeş,[d] Mustafa Durgun,[e] and Şükrü Beydemir[f, g]

Sulfonamide compounds known as human carbonic anhydrase (*h*CA) inhibitors are used in the treatment of many diseases such as epilepsy, antibacterial, glaucoma, various diseases. 1,3-diaryl-substituted triazenes and sulfaguanidine are used for therapeutic purposes in many drug structures. Based on these two groups, the synthesis of new compounds is important. In the present study, the novel 1,3-diaryltriazene-substituted sulfaguanidine derivatives (**SG1-13**) were synthesized and fully characterized by spectroscopic and analytic methods. Inhibitory effect of these compounds on the *h*CA I and hCA II was screened as in vitro. All the series of synthesized compounds have been identified as potential *h*CA isoenzymes inhibitory with K_I values in the range of 6.44±0.74-86.85±7.01 nM for *h*CA I and with K_I values in the range of 8.16±0.40-77.29±9.56 nM for *h*CA II. Moreover, the new series of compounds showed a more effective inhibition effect than the acetazolamide used as a reference. The possible binding positions of the compounds with a binding affinity to the *h*CA I and *h*CA II was demonstrated by in silico studies. In conclusion, compounds with varying degrees of affinity for *h*CA isoenzymes have been designed and as selective *h*CA inhibitors. These compounds may be potential alternative agents that can be used to treat or prevent diseases associated with glaucoma and *h*CA inhibition.

Introduction

Carbonic anhydrase (CA, EC 4.2.1.1), one of the enzymes containing zinc as a cofactor, is one of the most important enzymes involved in the cellular metabolism of living organisms. At least 15 CA isozymes have been mentioned in the tissues and cell fluids of many living things, especially mammals. The most active as catalysts for carbon dioxide hydration are CA II and CA IX. CA II is primarily found in red blood cells, but also in kidneys, lungs, eyes, etc.[1,2] When H^+ ions are produced as a result of hydration reactions, CA catalyzes the reversible reaction between carbon dioxide and bicarbonate and therefore, has a very important function in pH regulation in many tissues, organs and organisms.[3,4]

The existence of CA, which is common in organisms and consists of eight genetically different families (α, β, γ, δ, ζ, η, θ, and more recently ι), has been proven.[5–7] It has been reported that 15 different α-CA isoforms are involved in many physiological processes associated with the secretion of electrolytes, pH regulation, tumorigenesis, and biosynthetic processes in organisms.[8,9] Of the isoenzymes found in mammals, *h*CA I is among the major ones found in humans. *h*CA II, which is common in the eyes, has an important role in aqueous humor secretion as it affects the hydration of carbon dioxide and ion balance. Glaucoma is a group of diseases characterized by

[a] *Dr. S. Akocak, Dr. N. Lolak*
Department of Pharmaceutical Chemistry,
Faculty of Pharmacy,
Adıyaman University,
Adıyaman, 02040, Turkey
E-mail: sakocak@adiyaman.edu.tr

[b] *Dr. H. E. Duran*
Department of Medical Biochemistry,
Faculty of Medicine,
Kafkas University,
Kars, 36100, Turkey

[c] *Dr. M. Işık*
Department of Bioengineering,
Faculty of Engineering,
Bilecik Şeyh Edebali University,
Bilecik, 11230, Turkey
E-mail: mesut.isik@bilecik.edu.tr

[d] *Dr. C. Türkeş*
Department of Biochemistry,
Faculty of Pharmacy,
Erzincan Binali Yıldırım University,
Erzincan, 24002, Turkey

[e] *Dr. M. Durgun*
Department of Chemistry,
Faculty of Arts and Sciences,
Harran University,
Şanlıurfa, 63290, Turkey

[f] *Prof. Dr. Ş. Beydemir*
Department of Biochemistry,
Faculty of Pharmacy,
Anadolu University,
Eskişehir, 26470, Turkey

[g] *Prof. Dr. Ş. Beydemir*
Bilecik Şeyh Edebali University,
Bilecik, 11230, Turkey

elevated intraocular pressure (IOP) that causes irreversible blindness or visual field loss. Race, severe myopia, ocular hypertension, age and family history of glaucoma are among the risk factors for this disease.[10,11]

The activities of some metabolic enzymes may change as a result of disease, drug use and some metabolic disorders.[12,13] Physiologically, changes in the catalytic activity of *h*CA enzymes can occur pharmacologically with the use of antiglaucoma agents, diuretics, antiepileptics, antiobesity drugs, effective agents to treat high altitude sickness, anticancer/antimetastatic drugs targeting hypoxic tumors.[14,15] Many types of pharmacological effects are due to the fact that different isoforms of these *h*CAs are involved in various physiological processes and are targeted by such drugs. These isoforms are very similar in terms of their structural and functional properties.[16,17]

Sulfonamides and sulfamates have been reported to be potent inhibitors of most families of CAs, including α-class enzymes. Sulfonamides, which are of great importance in the pharmaceutical industry, are found as active ingredients in drugs that are widely used in the treatment or protection of many diseases. Aromatic/heterocyclic sulfonamides such as acetazolamide (AAZ) and sulfapyridine have been widely used for many years to understand the pathophysiology and treatment of different diseases such as epilepsy, antibacterial, glaucoma, various neurological/neuromuscular disorders, as well as control of acid-base imbalance or diuretic.[18,19] In clinical medicine, they are used primarily as carbonic anhydrase inhibitors, antibacterial, anticancer, antifungal, anti-obesity, diuretic, antiglaucoma and anticonvulsant agents.[20,21] Some systemic and topical sulfonamides used as antiglaucoma agents in the treatment of glaucoma have been used clinically for a long time and they regulate IOP as carbonic anhydrase inhibitors agents. It has been claimed that AAZ, a systemic compound, may be an effective way to reduce IOP by reducing aqueous humor secretion.[22] However, due to the fact that oral drugs may also inhibit other *h*CA isoenzymes in the body, different side effects have occurred. AAZ and other CA inhibitors have many side effects such as depression, nausea, anorexia, paresthesia, fatigue, weight loss, and acidosis and respiratory failure, among others.[23,24] It is important to conduct further research on CA I and CA II inhibitors and carefully evaluate the effects on *h*CA isoenzymes in the process of developing alternative drugs. This way, the risk of side effects can be minimized while achieving the desired effects of the medication. Therefore, it is important to design and develop new agents with varying degrees of affinity for each *h*CA isoenzyme to reduce these side effects.

1,3-diaryltriazenes have been preferred in many fields due to their easy synthesis and high efficiency. However, there are limited studies on the biological activities of 1,3-diaryltriazenes in the literature, apart from antioxidant, antidiabetic, antimicrobial, anti-inflammatory, wound healing, anti-dyslipidemic and insecticidal activities.[25–32] There are limited studies in the literature on the screening of inhibitory potentials of sulfaguanidine derivatives on *h*CA I and *h*CA II. In the study, the novel 1,3-diaryltriazene-substituted sulfaguanidine derivatives (**SG1**–**13**) were designed, synthesized and fully characterized by spectroscopic and analytic methods (FT-IR, ^{1}H-NMR, ^{13}C-NMR, and melting points). Our design strategy of these novel compounds were summarized in Figure 1. The inhibitory effect of the series of synthesized compounds (**SG1**–**13**) against *h*CA I and *h*CA II isoenzymes was investigated under *in vitro* and *in silico* studies.

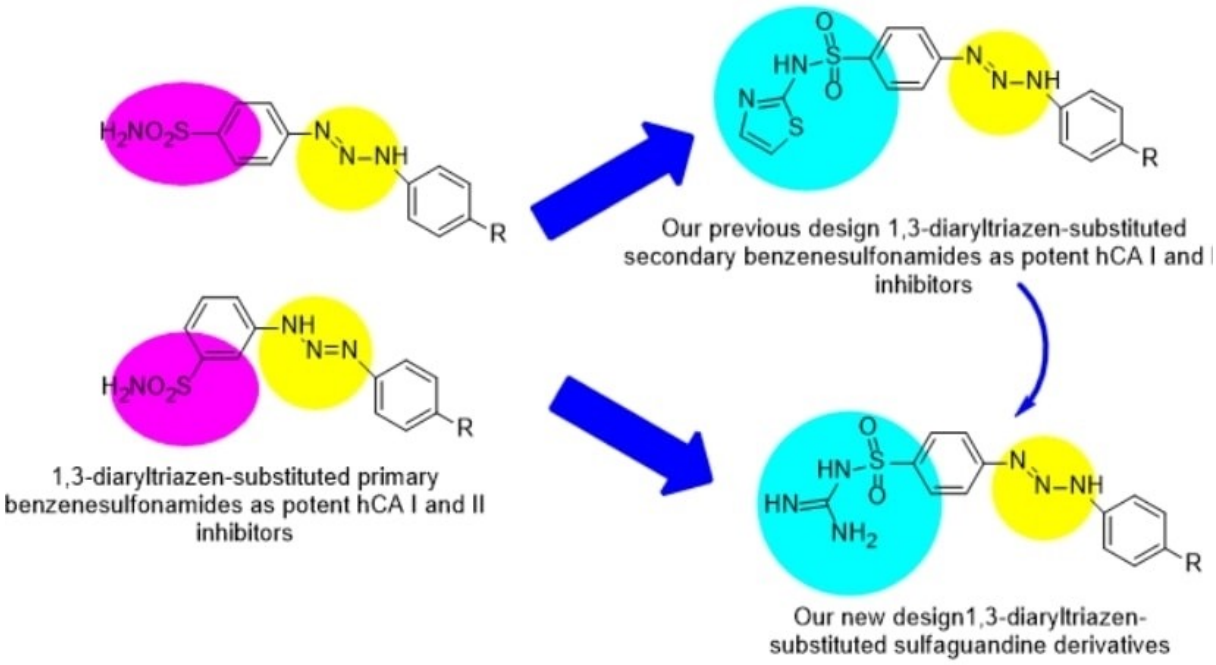

Figure 1. Our design strategy of newly synthesized 1,3-diaryltriazene-substituted sulfaguanidine derivatives as a potent hCA I and II inhibitors from our previous studies.

Results and Discussion

Biological study and structure-activity relationship (SAR) analysis

Sulfonamides (RSO_2NH_2), widely expressed as *h*CA inhibitors in the literature, have been used as antiglaucoma and diuretic drugs for a very long time. These molecules are used as active ingredients in many drug contents belonging to different clinical applications. It is known that *h*CA isoenzymes exist at high and different rates in many tissues and cell fluids of humans. This difference in cell fluid and tissues results in different selectivity of sulfamates and sulfonamides against different *h*CA isoenzymes.[25] Therefore, it is important to design alternative sulfonamide-based inhibitors with different selectivity towards *h*CAs.

In a study conducted in 2014, 1,2,4-triazole compounds with a benzenesulfonamide structure were synthesized and it was determined that the synthesized benzenesulfonamide compound inhibited the *h*CA II enzyme with K_I value of 6750 nM.[33] Benzyl *N*-(2-methoxybenzyl)sulfamoylcarbamate, one of the synthesis compounds made on synthesized benzylaminesulfamide carbamate and sulfamides, showed an inhibitory effect with a K_I value of 28.48 ± 0.01 nM for CA I, while *N*-(3,4,5-trimethoxybenzyl)sulfamide showed an inhibitory effect with K_I value of 112.01 ± 0.01 nM for *h*CA II.[34] In the study conducted with sulfanilamide derivatives carrying 1,3,5-triazinyl ring, the synthesized compound showed a high inhibitory effect on the *h*CA II enzyme with a K_I value of 12.5 nM.[35] In a study, some new 4-[2-(2-mercapto-4-oxo-4H-quinazolin-3-yl)-ethyl]-benzenesulfanamide derivatives were synthesized. Among the synthesized compound groups, it was determined that moderately (28.5–2954 nM K_I values) inhibition of CA I, derivatives carrying methyl, methoxy and halogen at positions 6,7,8 showed high inhibition of CA II and CA XII (0.62-12.4 nM).[36] A series of novel 1,3-diaryltriazene-substituted sulfathiazole moieties was synthesized. These synthesized novel derivatives were found to be effective inhibitor molecules with K_I values in the range of 450.37 ± 50.35–1,094.34 ± 111.37 nM for *h*CA I and 504.37 ± 57.22–1,205.36 ± 195.47 nM for *h*CA II.[37] The inhibition data obtained in the results of the study were found to be more effective than many results given in the literature. The results obtained from the inhibition data of the compounds, which consisted of synthesized sulfaguanidine derivatives, demonstrated a notably higher level of potency when compared to the findings reported in the previously mentioned literature studies. This indicates that the newly developed sulfaguanidine derivatives exhibit enhanced inhibitory effects on the target enzymes, surpassing the inhibitory potential of previously studied compounds.

In this study, the novel 1,3-diaryltriazene-substituted sulfaguanidine derivatives (**SG1**–**13**) were synthesized and the inhibitory effect of the its compounds against *h*CA I and *h*CA II isozymes was screened. In the series, all compounds (**SG1**–**13**) exhibited a high inhibitory effect on *h*CA I and *h*CA II isozymes as competitive and non-competitive inhibition types and at the nM level. The compounds have been identified as potential *h*CA isoenzymes inhibitory with K_I value in the range of 6.44 ± 0.74-86.85 ± 7.01 nM for *h*CA I and with K_I value in the range of 8.16 ± 0.40–77.29 ± 9.56 nM for *h*CA II. Moreover, the new series of synthesized compounds showed a more effective inhibition effect than AAZ (K_I 439.17 ± 9.30 nM for *h*CA I and K_I 98.28 ± 1.69 nM for *h*CA II) used as references against *h*CA I and *h*CA II. The compound **SG7** exhibits high inhibitory potential against *h*CA I with a K_I value of 6.44 ± 0.74 nM as competitive, while the **SG10** has a lower potency with a K_I value of 86.85 ± 7.01 nM as non-competitive. The compound **SG4** exhibits high inhibitory potential for *h*CA II with a K_I value of 11.85 ± 2.08 nM as competitive, while the **SG2** has a lower potency with a K_I value of 77.29 ± 9.56 nM as non-competitive (Table 1). These findings provide valuable insights into the design and optimization of sulfaguanidine derivatives as potential inhibitors of *h*CA I and II enzymes. The synthesized compounds demonstrated potent inhibitory effects and showed promise for further development as therapeutic agents targeting *h*CAs.

The structure-activity relationship (SAR) study revealed that the observed changes in the *h*CA I and *h*CA II inhibitory activity of sulfaguanidine-based analogs **SG1**–**13** are a result of the R variable substitution pattern on 1,3-diaryltriazene-substituted sulfaguanidine. The deviation in the *h*CA I and *h*CA II inhibitory potential of analogs **SG1**–**13** attributed to the different functional groups of the R variable substitution pattern on 1,3-diaryltriazene-substituted sulphaguanidine. The order of inhibition potentials of the compounds on the *h*CA I was **SG10** < **SG9** < **SG1** < **SG2** < **SG4** < **SG11** < **SG12** < **SG6** < **SG5** < **SG13** < **SG8** < **SG3** < **SG7**. According to the results, the −4 acetyl (**SG7**) substitution in the 1,3-diaryltriazene ring shows a greater increase in *h*CA I inhibition than the others. Again, substitutions of −4Cl (**SG3**), −4MeO (**SG8**) and −3,4diCl (**SG13**) in the ring containing the R group and others caused an increase in *h*CA I inhibitory activity (Scheme 1). The order of inhibition potentials of the compounds on the *h*CA II was **SG2** < **SG1** < **SG7** < **SG6** < **SG8** < **SG12** < **SG3** < **SG11** < **SG5** < **SG9** < **SG13** < **SG4** < **SG10**. Substitution of −2,3,4,5,6F (**SG10**) on the 1,3-diaryltriazene ring produced a significant increase in the *h*CA II inhibitory activity of compound **10**. On the other hand, substitutions of −4CN (**SG4**), −3,4diCl (**SG13**) and -BuO (**SG9**) in the ring containing the R group and others also caused an increase in *h*CA II inhibitory activity. As the active group, substitutions of −3,4diCl (**SG13**) have been shown to increase inhibition of *h*CA I and *h*CA II (Scheme 1).

Computational studies

The present study investigated the binding patterns of newly synthesized 1,3-diaryltriazene-substituted sulfaguanidine derivatives (**SG1-13**) using X-ray crystallographic structures of the *h*CA I (PDB ID 1AZM) and *h*CA II (PDB ID 3 V2 J) isoforms. The native ligand AZM (AAZ, 5-acetamido-1,3,4-thiadiazole-2-sulfonamide) was re-docked in the enzyme binding sites to validate the docking methodology. The docking poses of the co-crystalized ligands exhibited minimal root-mean-square deviation (RMSD) values of 0.21 Å and 0.14 Å for 1AZM and 3 V2 J,

Table 1. Inhibition data of carbonic anhydrase I and II isozymes with the novel 1,3-diaryltriazene-substituted sulfaguanidine derivatives (**SG1**–**13**) and standard drug acetazolamide.

Compound ID	*h*CA I			*h*CA II		
	K_I (nM)[a]	R^2	Inhibition type	K_I (nM) [a]	R^2	Inhibition type
SG1	42.47 ± 3.66	0.9893	Competitive	58.35 ± 8.52	0.9713	Competitive
SG2	23.58 ± 2.88	0.9797	Competitive	77.29 ± 9.56	0.9649	Noncompetitive
SG3	9.21 ± 1.21	0.9757	Competitive	21.35 ± 3.38	0.9624	Competitive
SG4	21.73 ± 2.79	0.9768	Competitive	11.85 ± 2.08	0.9611	Competitive
SG5	13.21 ± 1.51	0.9830	Competitive	19.53 ± 1.93	0.9875	Competitive
SG6	15.69 ± 2.05	0.9761	Competitive	30.31 ± 1.84	0.9815	Noncompetitive
SG7	6.44 ± 0.74	0.9817	Competitive	49.98 ± 4.27	0.9626	Noncompetitive
SG8	9.73 ± 1.58	0.9659	Competitive	27.23 ± 1.80	0.9788	Noncompetitive
SG9	83.96 ± 7.04	0.9731	Noncompetitive	16.44 ± 1.57	0.9877	Competitive
SG10	86.85 ± 7.01	0.9675	Noncompetitive	8.16 ± 0.40	0.9894	Noncompetitive
SG11	20.97 ± 1.91	0.9886	Competitive	19.70 ± 2.32	0.9795	Competitive
SG12	17.66 ± 2.45	0.9748	Competitive	25.16 ± 2.30	0.9879	Competitive
SG13	12.61 ± 1.48	0.9827	Competitive	14.41 ± 1.41	0.9864	Competitive
AAZ[b]	439.17 ± 9.30	0.9990	Noncompetitive	98.28 ± 1.69	0.9992	Noncompetitive

[a] The test results were expressed as means of triplicate assays ± SEM. [b] Acetazolamide.

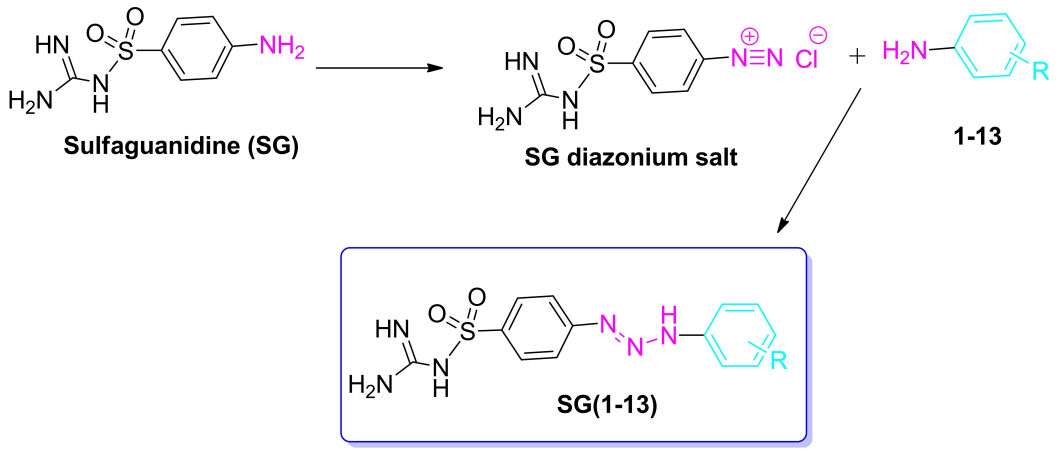

R = { -H (**SG-1**), -4F (**SG-2**), -4Cl (**SG-3**), -4CN (**SG-4**),-4COOH (**SG-5**), -2CN (**SG-6**), -4Acetyl (**SG-7**), -4MeO (**SG-8**), 4BuO (**SG-9**), -2,3,4,5,6F (**SG-10**), -3NO_2 (**SG-11**), -3,4diMeO (**SG-12**), -3,4diCl (**SG-13**), }

Scheme 1. General synthetic route for the synthesis of the novel 1,3-diaryltriazene-substituted sulfaguanidine derivatives **SG1**–**13**. Reagent and conditions: (i) H_2O, HCl, $NaNO_2$, 0–5 °C, 30 min, (ii) Substituted aromatic anilines (**1**–**13**), MeOH, H_2O, sodium acetate, 0–5 °C, 3 h, r.t., overnight.

respectively, and successfully reproduced all essential interactions. The validated setup was subsequently employed to investigate the binding mechanisms of the synthesized derivatives in the active sites of *h*CAs. The most potent inhibitors, **SG7** (for *h*CA I) and **SG4** (for *h*CA II), displayed strong binding affinity to the *h*CA isoforms, with predicted docking scores of −4.48 kcal/mol and −3.00 kcal/mol, respectively. The newly developed derivatives exhibited comparable binding patterns in the *h*CAs, including accommodation of the sulfonamide moiety in the binding site by hydrogen bonding with gatekeeper residues Thr199 (distances of 1.89 Å for *h*CA I) and Thr200 (distance of 2.37 Å for *h*CA II) (Figure 2 and 3). Additionally, in *h*CA II, the carbonyl moiety interacted via hydrogen bonding with Tyr204 in the center of the active site at a distance of 1.79 Å. The observed differences in affinity and selectivity of the novel 1,3-diaryltriazene-substituted sulfaguanidines for each *h*CA were attributed to their distinct structural variations, resulting in unique steric and electronic properties. Furthermore, it is a widely recognized fact that a number of potential drugs have proven unsuccessful in clinical trials due to their deficient pharmacokinetic profiles, leading to a failure to ultimately enter the market. Incorporating *in silico* absorp-

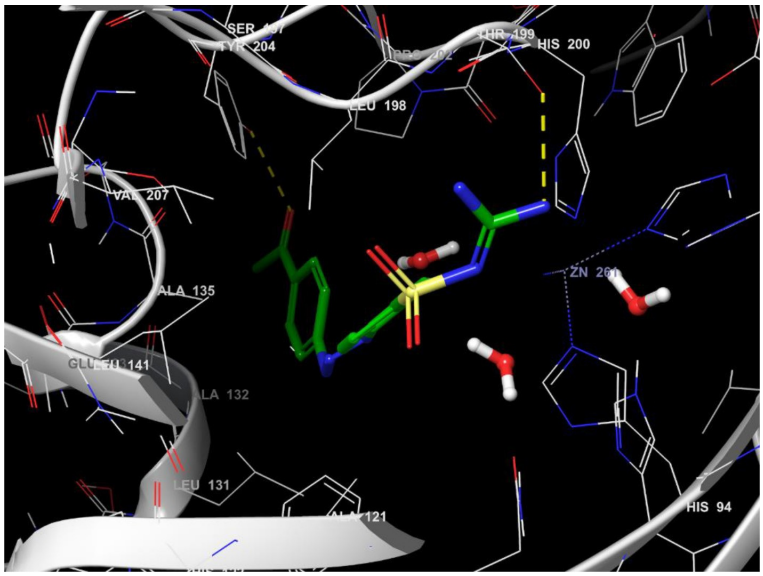

A)

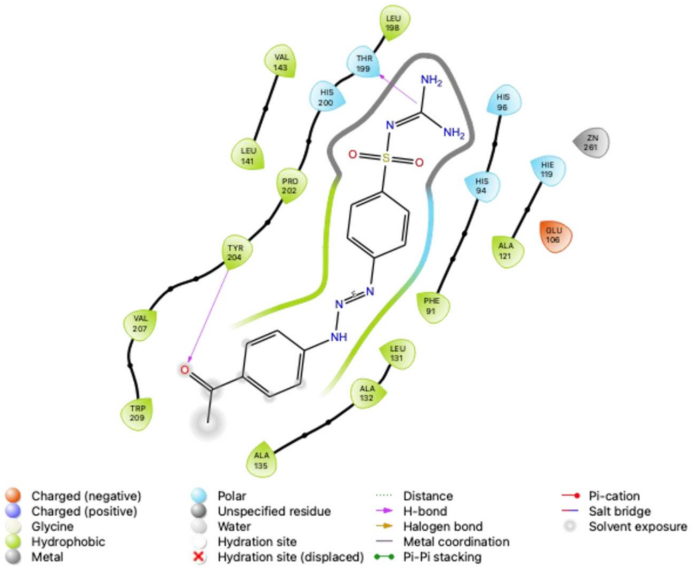

B)

Figure 2. Molecular docking of carbonic anhydrase I isoenzyme (PDB code: 1AZM) with compound **SG7** (4-(3-(4-acetylphenyl)triaz-1-en-1-yl)-*N*-carbamimidoylbenzenesulfonamide). (**A**) 3D docking pose of compound **SG7** within the binding pocket of 1AZM. In the 3D panel, only the interacting amino acids are demonstrated for clarity. (**B**) 2D binding interaction of 1AZM with compound **SG7**.

tion, distribution, metabolism, elimination/excretion, and toxicity (ADME/T) predictions into the early stages of drug discovery programs has become increasingly prevalent, as this approach entails lower costs and time demands than traditional experimental ADME/T profiling methods. In this direction, the ADME/T properties were predicted by the Qikprop module,[38] as shown in Table 2. All the derivatives (**SG1**–**13**) were found to be within the permissible limits of Lipinski's[39] and Jorgensen's[40] rules.

Conclusions

In conclusion, this study focused on the synthesis and evaluation of novel 1,3-diaryltriazene-substituted sulfaguanidine derivatives (**SG1**–**13**) as inhibitors of *h*CA I and II isozymes. The synthesized compounds exhibited high inhibitory effects on both isozymes, acting through competitive and non-competitive inhibition mechanisms at the nanomolar level. Notably, the newly developed derivatives showed greater inhibitory potency than the reference compound AAZ against *h*CA I and *h*CAII. The structure-activity relationship analysis revealed that the substitution pattern of the R variable on the 1,3-diaryltriazene-substituted sulfaguanidine influ-

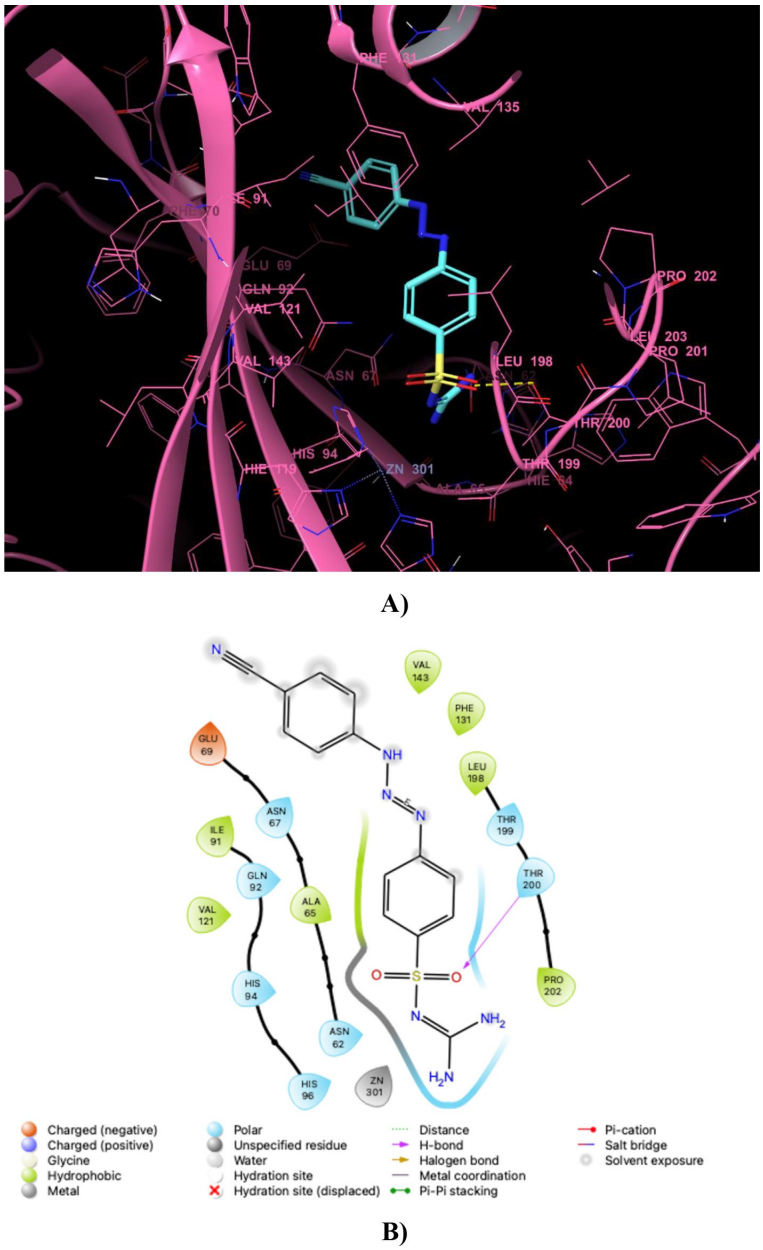

Figure 3. Molecular docking of carbonic anhydrase II isoenzyme (PDB code: 3 V2 J) with compound **SG4** (*N*-carbamimidoyl-4-(3-(4-cyanophenyl)triaz-1-en-1-yl)benzenesulfonamide). (**A**) 3D docking pose of compound **SG4** within the binding pocket of 3 V2 J. In the 3D panel, only the interacting amino acids are demonstrated for clarity. (**B**) 2D binding interaction of 3 V2 J with compound **SG4**.

enced the inhibitory activity on both *h*CA I and II. Computational docking studies supported the binding affinity of the most potent inhibitors (**SG7** for *h*CA I and **SG4** for *h*CA II) by successfully reproducing essential interactions in the active sites of the target enzymes. The observed differences in affinity and selectivity among the derivatives were attributed to their distinct structural variations, resulting in unique steric and binding properties. Overall, the newly synthesized sulfaguanidine derivatives hold promise as potential inhibitors of *h*CA I and II, highlighting their potential for further development in the field of enzyme inhibition. Further research is needed on the design and development of alternative potential agents that that can be used to treat or prevent diseases associated with glaucoma and *h*CA inhibition in the future.

Experimental Section

General synthetic procedure for the preparation of 1,3-diaryltriazene-substituted sulfaguanidine derivatives (SG1–13)

The compounds (**SG1–13**) were synthesized according to our previous studies by using our optimized reaction conditions. Briefly, a mixture of sulfaguanidine (**SG**) (5 mmol) in 1.5 ml of conc. hydrochloric acid

Table 2. ADME/T related parameters[a] of with the the novel 1,3-diaryltriazene-substituted sulfaguanidine derivatives **SG1-13** and standard drug acetazolamide.

Compound ID	CNS	MW	Dipole	Volume	donorHB	accptHB	QPlogPoct	QPlogPw	QPlogPo/w	QPlogS	QPPCaco	QPlogBB	QPlogKp	Metab	QPlogKhsa	HOA	PSA	Rule of Five	Rule of Three
SG1	−2	318.35	7.46	987.85	3	7.5	20.44	15.66	0.80	−3.59	38.74	−2.41	−4.42	5	−0.38	60.06	144.27	0	0
SG2	−2	336.34	8.03	1003.79	3	7.5	20.81	15.44	1.03	−3.93	38.76	−2.32	−4.55	4	−0.35	61.37	144.28	0	0
SG3	−2	352.80	8.00	1032.08	3	7.5	21.23	15.42	1.27	−4.27	38.70	−2.29	−4.59	4	−0.29	62.79	144.27	0	0
SG4	−2	343.36	10.29	1052.98	3	9	22.65	17.26	0.08	−4.64	8.06	−3.34	−5.77	4	−0.52	43.65	170.07	0	1
SG5	−2	362.36	7.58	1070.03	4	9.5	24.01	19.27	0.13	−3.58	0.98	−3.67	−6.49	4	−0.72	14.57	194.07	1	1
SG6	−2	343.36	10.56	1050.70	3	9	22.69	17.24	0.14	−4.59	9.69	−3.23	−5.60	5	−0.52	45.40	169.15	0	1
SG7	−2	360.39	9.64	1110.79	3	9.5	23.22	17.45	0.32	−3.91	12.25	−3.17	−5.54	4	−0.47	48.29	173.33	0	1
SG8	−2	348.38	7.84	1063.72	3	8.3	21.37	15.89	0.90	−3.82	38.62	−2.54	−4.52	5	−0.38	60.60	152.47	0	0
SG9	−2	390.46	7.79	1260.28	3	8.3	23.07	15.51	2.03	−5.16	38.52	−3.02	−4.24	5	−0.08	67.19	151.94	0	0
SG10	−2	408.31	7.56	1066.00	3	7.5	21.67	14.77	1.89	−5.13	46.38	−1.93	−4.79	4	−0.22	67.84	144.39	0	0
SG11	−2	363.35	8.97	1061.60	3	8.5	22.18	16.79	0.11	−3.78	4.56	−3.60	−6.34	6	−0.42	26.42	189.26	1	1
SG12	−2	378.41	7.28	1138.82	3	9	22.11	16.15	0.99	−4.09	38.54	−2.68	−4.62	6	−0.37	61.10	159.93	0	0
SG13	−2	387.24	8.15	1072.65	3	7.5	21.89	15.23	1.68	−4.85	38.60	−2.18	−4.73	4	−0.20	65.18	144.30	0	0
AAZ[b]	−2	222.24	10.76	634.43	3	9	17.57	15.15	−1.75	−1.55	36.88	−1.74	−5.90	1	−0.97	44.77	134.97	0	0

[a] CNS, Central nervous system activity (−2 inactive, +2 active); MW, molecular weight of the compound (130.00 - 725.00); Dipole, computed dipole moment of the compound (1.00 - 12.50); Volume, total solvent-accessible volume in cubic angstroms using a probe with a 1.4 Å Radius (500.00 - 2000.00); donorHB, estimated number of hydrogen bonds that would be donated by the solute to water molecules in an aqueous solution (0 - 6); accptHB, estimated number of hydrogen bonds that would be accepted by the solute from water molecules in an aqueous solution (2 - 20); QPlogPoct, octanol/gas partition coefficient (8.00 - 35.00); QPlogPw, water/gas partition coefficient (4.00 - 45.00); QPlogPo/w, octanol/water partition coefficient (−2.00 - 6.50); QPlogS, aqueous solubility (−6.50 - 0.50); QPPCaco, apparent Caco-2 cell permeability in nm/sec (<25 poor, great>500); QPlogBB, brain/blood partition coefficient (−3.00 - 1.20); QPlogKp, skin permeability (−8.00 - −1.00); Metab, number of likely metabolic reactions (1 - 8); QPlogKhsa, prediction of binding to human serum albumin (−1.50 - 1.50); HOA; human oral absorption (<25% poor, high>80%); PSA, van der Waals surface area of polar nitrogen and oxygen atoms (7.00 - 200.00); Rule of Five, number of violations of Lipinski's rule of five (max. 4); Rule of Three, number of violations of Jorgensen's rule of three (max. 3). [b] Acetazolamide.

and 10 ml of water was cooled to 0–5 °C, sodium nitrite (7 mmol) in 5 ml of water was added dropwise to this solution during 15–20 min under continuous stirring. The mixture was stirred around 30 min at 0–5 °C, and diazonium solution was added to aniline solution (prepared by 5 mmol substituted anilines in 5 ml of MeOH) by adjusting the pH around 6–7 with simultaneous addition of saturated sodium acetate in water. Then, the reaction mixture was stirred 3 h. at 0–5 °C and overnight at room temperature in dark. Reactions were monitored through IR spectroscopy and TLC. The obtained colorful solid was filtered off, washed several times with cold water, the crystallized from suitable solvents and dried under vacuum. The chemical structures of obtained pure products **SG1**–**13** were characterized by spectroscopic and analytic methods (FT-IR, ^{1}H-NMR, ^{13}C-NMR, and melting points).

N-Carbamimidoyl-4-(3-phenyltriaz-1-en-1-yl)benzenesulfonamide (SG1)

Yield: 67%; Color: light orange solid; Melting Point: 217–218 °C; Anal. calc. for $C_{13}H_{14}N_6O_2S$ (318.36 g/mol) (%): C, 49.05; H, 4.43; N, 26.40; S, 10.07, Found (%): C, 49.01; H, 4.46; N, 26.45; S, 10.03. FT-IR (cm^{-1}): 3439, 3442, 3235, 3194 (NH), 1738, 1624, 1253, 1131 (symmetric) (S=O), 1092; ^{1}H-NMR ((D_6)DMSO, 400 MHz, δ ppm): 12.70 (s, 1H, –NH–), 7.75 (d, J = 8.4, 2H, Ar–H), 7.51–7.41 (m, 6H, Ar–H), 7.24 (t, 2H, Ar–H), 6.71 (s, 4H, guanidine); ^{13}C-NMR ((D_6)DMSO, 100 MHz, δ ppm): 158.55, 140.23, 129.73, 127.65, 122.03, 113.67, 103.42.

N-Carbamimidoyl-4-(3-(4-fluorophenyl)triaz-1-en-1-yl)benzenesulfonamide (SG2)

Yield: 78%; Color: cream solid; Melting Point: 211–213 °C; Anal. calc. for $C_{13}H_{13}FN_6O_2S$ (336.35 g/mol) (%): C, 46.42; H, 3.90; N, 24.99; S, 9.53, Found (%): C, 46.39; H, 3.91; N, 25.04; S, 9.58. FT-IR (cm^{-1}): 3467, 3417, 3212, 3189 (NH), 1738, 1617, 1249, 1134 (symmetric) (S=O), 1090; ^{1}H-NMR ((D_6)DMSO, 400 MHz, δ ppm): 12.70 (br. s, 1H, –NH–), 7.74 (d, J = 8.8, 2H, Ar–H), 7.58–7.54 (m, 2H, Ar–H), 7.43 (d, J = 8.4, 2H, Ar–H), 7.27 (t, 2H, Ar–H), 6.87 (s, 4H, guanidine); ^{13}C-NMR ((D_6)DMSO, 100 MHz, δ ppm): 162.35, 158.70, 145.87, 144.91, 139.32, 127.68, 121.86, 116.62, 115.38.

N-Carbamimidoyl-4-(3-(4-chlorophenyl)triaz-1-en-1-yl)benzenesulfonamide (SG3)

Yield: 83%; Color: cream solid; Melting Point: 199–200 °C; Anal. calc. for $C_{13}H_{13}ClN_6O_2S$ (352.80 g/mol) (%): C, 44.26; H, 3.71; N, 23.82; S, 9.09, Found (%): C, 44.24; H, 3.72; N, 23.86; S, 9.05. FT-IR (cm^{-1}): 3473, 3412, 3196 (NH), 1738, 1249, 1134 (symmetric) (S=O), 1090; ^{1}H-NMR ((D_6)DMSO, 400 MHz, δ ppm): 12.80 (s, 1H, –NH–), 7.75 (d, J = 7.4, 2H, Ar–H), 7.55–7.40 (m, 6H, Ar–H), 6.69 (s, 4H, guanidine); ^{13}C-NMR ((D_6)DMSO, 100 MHz, δ ppm): 163.51, 158.53, 143.92, 129.61, 127.67, 123.00, 113.36, 104.03.

N-Carbamimidoyl-4-(3-(4-cyanophenyl)triaz-1-en-1-yl)benzenesulfonamide (SG4)

Yield: 68%; Color: yellow solid; Melting Point: 195–196 °C; Anal. calc. for $C_{14}H_{13}N_7O_2S$ (343.37 g/mol) (%): C, 48.97; H, 3.82; N, 28.56; S, 9.34, Found (%): C, 48.92; H, 3.85; N, 28.58; S, 9.30. FT-IR (cm^{-1}): 3427, 3338, 3187 (NH), 2233 (CN), 1738, 1634, 1252, 1132 (symmetric) (S=O), 1104; ^{1}H-NMR ((D_6)DMSO, 400 MHz, δ ppm): 7.83–7.75 (m, 4H, Ar–H), 7.60–7.54 (m, 4H, Ar–H), 6.95 (s, 4H, guanidine); ^{13}C-NMR ((D_6)DMSO, 100 MHz, δ ppm): 158.79, 149.32, 141.99, 134.17, 133.86, 127.547 119.23, 117.63, 113.84, 105.88.

N-Carbamimidoyl-4-(3-(4-carboxyphenyl)triaz-1-en-1-yl)benzensulfonamide (SG5)

Yield: 63%; Color: dark yellow solid; Melting Point: 185–186 °C; Anal. calc. for $C_{14}H_{14}N_6O_4S$ (362.36 g/mol) (%): C, 46.40; H, 3.89; N, 23.19; S, 8.85, Found (%): C, 46.38; H, 3.91; N, 23.26; S, 8.79. FT-IR (cm^{-1}): 3445, 3377, 3222 (NH and OH), 1716, 1627, 1249, 1135 (symmetric) (S=O), 1096; ^{1}H-NMR ((D_6)DMSO, 400 MHz, δ ppm): 12.88 (br. s, 2H, –NH- and -OH), 7.98 (d, J = 7.6, 2H, Ar–H), 7.81 (d, J = 8.0, 2H, Ar–H), 7.58 (d, J = 8.0, 2H, Ar–H), 7.53 (d, J = 8.0, 2H, Ar–H), 6.74 (s, 4H, guanidine); ^{13}C-NMR ((D_6)DMSO, 100 MHz, δ ppm): 183.07, 167.48, 158.38, 148.52, 131.40, 127.57, 118.62, 116.68.

N-Carbamimidoyl-4-(3-(2-cyanophenyl)triaz-1-en-1-yl)benzenesulfonamide (SG6)

Yield: 68%; Color: orange solid; Melting Point: 243–244 °C; Anal. calc. for $C_{14}H_{13}N_7O_2S$ (343.37 g/mol) (%): C, 48.97; H, 3.82; N, 28.56; S, 9.34, Found (%): C, 48.93; H, 3.86; N, 28.60; S, 9.31. FT-IR (cm^{-1}): 3418, 3336, 3240, 3190 (NH), 2220 (CN), 1737, 1639, 1255, 1132 (symmetric) (S=O), 1092; ^{1}H-NMR ((D_6)DMSO, 400 MHz, δ ppm): 8.32 (s, 1H, –NH–), 7.86 (d, J = 7.6, 1H, Ar–H), 7.81 (d, J = 8.0, 1H, Ar–H), 7.77–7.69 (m, 3H, Ar–H), 7.51 (d, J = 8.0, 2H, Ar–H), 7.40 (t, 1H, Ar–H), 6.76 (s, 4H, guanidine); ^{13}C-NMR ((D_6)DMSO, 100 MHz, δ ppm): 158.59, 152.34, 139.64, 134.50, 134.19, 127.71, 127.32, 118.81, 118.19, 115.40, 106.78.

N-Carbamimidoyl-4-(3-(4-acetylphenyl)triaz-1-en-1-yl)benzenesulfonamide (SG7)

Yield: 81%; Color: light orange solid; Melting Point: 225–226 °C; Anal. calc. for $C_{15}H_{16}N_6O_3S$ (360.39 g/mol) (%): C, 49.99; H, 4.48; N, 23.32; S, 8.90, Found (%): C, 49.95; H, 4.46; N, 23.35; S, 8.88. FT-IR (cm^{-1}): 3444, 3339, 3211 (NH), 1736, 1630, 1256, 1135 (symmetric) (S=O), 1098; ^{1}H-NMR ((D_6)DMSO, 400 MHz, δ ppm): 13.00 (br. s, 1H, –NH–), 8.00 (d, J = 8.4, 2H, Ar–H), 7.80 (d, J = 8.0, 2H, Ar–H), 7.59 (d, J = 8.0, 2H, Ar–H), 7.51 (d, J = 8.0, 2H, Ar–H), 6.76 (s, 4H, guanidine), 2.56 (s, 3H, -CH_3); ^{13}C-NMR ((D_6)DMSO, 100 MHz, δ ppm): 196.99, 160.81, 158.62, 141.59, 133.23, 130.47, 127.53, 118.92, 116.95, 112.95, 26.97.

N-Carbamimidoyl-4-(3-(4-methoxyphenyl)triaz-1-en-1-yl)benzenesulfonamide (SG8)

Yield: 75%; Color: brown solid; Melting Point: 182–183 °C; Anal. calc. for $C_{14}H_{16}N_6O_3S$ (348.38 g/mol) (%): C, 48.27; H, 4.63; N, 24.12; S, 9.20, Found (%): C, 48.24; H, 4.61; N, 24.15; S, 9.18. FT-IR (cm^{-1}): 3425, 3327 (NH), 1736, 1627, 1246, 1130 (symmetric) (S=O), 1087; ^{1}H-NMR ((D_6)DMSO, 400 MHz, δ ppm): 12.44 (br. s, 1H, –NH–), 7.70 (d, J = 7.6, 2H, Ar–H), 7.50 (d, J = 7.6, 2H, Ar–H), 7.37 (d, J = 7.6, 2H, Ar–H), 7.01 (d, J = 8.0, 2H, Ar–H), 6.81 (s, 4H, guanidine), 3.80 (s, 3H, –OCH_3); ^{13}C-NMR ((D_6)DMSO, 100 MHz, δ ppm): 158.91, 144.53, 138.59, 127.70, 122.03, 114.98, 114.32, 103.73, 100.71, 55.85.

N-Carbamimidoyl-4-(3-(4-butoxyphenyl)triaz-1-en-1-yl)benzenesulfonamide (SG9)

Yield: 71%; Color: dark orange solid; Melting Point: 189–190 °C; Anal. calc. for $C_{17}H_{22}N_6O_3S$ (390.46 g/mol) (%): C, 52.29; H, 5.68; N, 21.52; S, 8.21, Found (%): C, 52.26; H, 5.66; N, 21.56; S, 8.17. FT-IR (cm^{-1}): 3480, 3417, 3338, 3231 (NH), 1738, 1628, 1233, 1131 (symmetric) (S=O), 1090; ^{1}H-NMR ((D_6)DMSO, 400 MHz, δ ppm): 12.43 (s, 1H, –NH–), 7.71 (d, J = 7.6, 2H, Ar–H), 7.49 (d, J = 7.6, 2H, Ar–H), 7.37 (d, J = 7.6, 2H, Ar–H), 6.99 (d, J = 8.0, 2H, Ar–H), 6.67 (s, 4H, guanidine), 4.00 (s, 2H,

–OCH_3CH_2CH_2CH_3), 1.70 (m, 2H, –OCH$_3$CH_2CH_2CH$_3$), 1.44 (m, 2H, –OCH$_3$CH$_2$CH_2CH$_3$), 0.95 (t, 3H, –OCH$_3$CH$_2$CH$_2$CH_3); ^{13}C-NMR ((D$_6$)DMSO, 100 MHz, δ ppm): 158.48, 145.60, 140.24, 133.23, 127.74, 115.49, 104.03, 67.91, 31.22, 19.20, 14.17.

N-Carbamimidoyl-4-(3-(perfluorophenyl)triaz-1-en-1-yl)benzenesulfonamide (SG10)

Yield: 55 %; Color: brown solid; Melting Point: 273–274 °C; Anal. calc. for $C_{13}H_9F_5N_6O_2S$ (408.31 g/mol) (%): C, 38.24; H, 2.22; N, 20.58; S, 7.85, Found (%): C, 38.20; H, 2.17; N, 20.65; S, 7.79. FT-IR (cm^{-1}): 3471, 3438, 3227 (NH), 1738, 1633, 1248, 1135 (symmetric) (S=O), 1098; ^{1}H-NMR ((D$_6$)DMSO, 400 MHz, δ ppm): 8.04 (d, J = 8.4, 2H, Ar–H), 7.98 (d, J = 7.6, 2H, Ar–H), 6.97 (br. s, 4H, guanidine); ^{13}C-NMR ((D$_6$)DMSO, 100 MHz, δ ppm): 173.99, 159.14, 152.20, 146.58, 137.23, 127.47, 125.61.

N-Carbamimidoyl-4-(3-(3-nitrophenyl)triaz-1-en-1-yl)benzenesulfonamide (SG11)

Yield: 65 %; Color: yellow solid; Melting Point: 230–231 °C; Anal. calc. for $C_{13}H_{13}N_7O_4S$ (363.35 g/mol) (%): C, 42.97; H, 3.61; N, 26.98; S, 8.82, Found (%): C, 42.91; H, 3.64; N, 27.01; S, 8.78. FT-IR (cm^{-1}): 3480, 3450, 3376, 3227 (NH), 1738, 1634, 1246, 1131 (symmetric) (S=O), 1093; ^{1}H-NMR ((D$_6$)DMSO, 400 MHz, δ ppm): 8.18 (s, 1H, Ar–H), 8.01 (d, J = 7.6, 1H, Ar–H), 7.91 (d, J = 7.6, 1H, Ar–H), 7.80 (d, J = 8.4, 2H, Ar–H), 7.69 (t, 1H, Ar–H), 7.54 (d, J = 8.0, 2H, Ar–H), 6.90 (s, 4H, guanidine); ^{13}C-NMR ((D$_6$)DMSO, 100 MHz, δ ppm): 158.72, 149.34, 148.16, 147.45, 140.89, 131.22, 127.63, 125.02, 119.84, 117.49, 112.65.

N-Carbamimidoyl-4-(3-(3,4-dimethoxyphenyl)triaz-1-en-1-yl)benzenesulfonamide (***SG12***)

Yield: 82 %; Color: dark purplish red solid; Melting Point: 272–273 °C; Anal. calc. for $C_{15}H_{18}N_6O_4S$ (378.41 g/mol) (%): C, 47.61; H, 4.79; N, 22.21; S, 8.47, Found (%): C, 47.58; H, 4.75; N, 22.26; S, 8.41. FT-IR (cm^{-1}): 3425, 3355, 3215 (NH), 1737, 1621, 1252, 1120 (symmetric) (S=O), 1093; ^{1}H-NMR ((D$_6$)DMSO, 400 MHz, δ ppm): 8.33 (s, 1H, Ar–H), 7.89 (d, J = 8.4, 2H, Ar–H), 7.82 (d, J = 8.4, 2H, Ar–H), 7.17 (s, 2H, Ar–H), 7.10–6.69 (m, 4H, guanidine), 6.46 (s, 1H, Ar–H), 3.81 (s, 3H, –OCH$_3$), 3.72 (s, 3H, –OCH$_3$); ^{13}C-NMR ((D$_6$)DMSO, 100 MHz, δ ppm): 159.67, 155.78, 154.67, 144.80, 144.28, 141.97, 129.92, 127.05, 121.98, 104.40, 99.31, 56.10, 55.98.

N-Carbamimidoyl-4-(3-(3,4-dichlorophenyl)triaz-1-en-1-yl)benzenesulfonamide (***SG13***)

Yield: 78 %; Color: dark yellow solid; Melting Point: 225–226 °C; Anal. calc. for $C_{13}H_{12}Cl_2N_6O_2S$ (387.24 g/mol) (%): C, 40.32; H, 3.12; N, 21.70; S, 8.28, Found (%): C, 40.29; H, 3.14; N, 21.73; S, 8.23. FT-IR (cm^{-1}): 3434, 3353, 3235, 3195 (NH), 1738, 1625, 1234, 1127 (symmetric) (S=O), 1092; ^{1}H-NMR ((D$_6$)DMSO, 400 MHz, δ ppm): 8.32 (s, 1H, Ar–H), 7.75 (d, J = 8.4, 2H, Ar–H), 7.68 (s, 1H, Ar–H), 7.63 (d, J = 8.4, 1H, Ar–H), 7.50 (d, J = 8.4, 2H, Ar–H), 7.44 (d, J = 8.4, 1H, Ar–H), 6.96 (s, 4H, guanidine); ^{13}C-NMR ((D$_6$)DMSO, 100 MHz, δ ppm): 158.96, 147.58, 147.38, 140.42, 132.31, 131.61, 127.55, 127.34, 120.18, 119.54, 117.01.

hCA isoenzymes activity

First, the purification of *h*CA isoenzymes (*h*CA I and *h*CA II) from human erythrocytes was performed according to the modified procedure described in the literature.[41,42] In the inhibition studies, according to our previous studies, the esterase activities of *h*CA isoforms were determined by the *p*-nitrophenyl acetate that used as a substrate converted by both isoforms to the *p*-nitrophenolate ion in this technique.[43–45]

In vitro inhibition studies

The inhibition effects of the novel 1,3-diaryltriazene-substituted sulfaguanidine derivatives (**SG1-13**) were determined with different inhibitor concentrations (at least five) against *h*CA isoenzymes (*h*CA I and *h*CA II). The IC_{50} of the derivatives was calculated from Activity (%)-[Sulfaguanidine Derivative] graphs for each derivatives. The inhibition types and K_i values were found by Lineweaver and Burk's curves.[46,47]

Computational studies

The Protein Data Bank (PDB) was used to retrieve the *h*CA I and II complexes (PDB IDs: 1AZM, 2.0 Å resolution and 3 V2 J, 1.70 Å resolution, respectively) with acetazolamide (AAZ or AZM).[48] There were 260 residues in each PDB structure. The Schrödinger Suite's (2022-3) Protein Preparation Wizard[49] was used to prepare the enzymes.[50,51] At a pH of 7.4, Propka was used to optimize hydrogen bond assignments, and a sampling of water orientations was finished.[52] The final phase of the enzyme preparation was restricted minimization with the OPLS4 force field.[53] LigPrep[54] and the OPLS4[55] force field were used to prepare and minimize the 3D structures of the novel 1,3-diaryltriazene-substituted sulfaguanidine derivatives (**SG1**–**13**). AZM was used as the centroid to create a grid,[56] and the glide extra precision (XP) docking procedure[57–59] was used as in our previous studies.[60] Flexible ligand sampling was used, and the docking score included Epik state penalties.[61,62] Also, MM-GBSA predicts[63–65] were carried out in the VSGB energy model and OPLS4 force field. Maestro[66] was utilized to produce molecular docking images. Also, ADME/T properties of the derivatives (**SG1**–**13**) were calculated using the Qikprop tool.[67]

Statistical studies

Analysis of the data and drawing of graphs were realized using GraphPad Prism version 8 for Mac (GraphPad Software, La Jolla California USA). The fit of enzyme inhibition models was compared using the extra sum-of-squares *F* test and the AICc approach. The results were exhibited as mean ± standard error of the mean (95 % confidence intervals). Differences between data sets were considered statistically significant when the *p*-value was less than 0.05.

Acknowledgements

This work was supported by the Research Fund of Anadolu University (grant number 2102 S003).

Conflict of Interests

The authors declare no conflict of interest.

Data Availability Statement

The data that support the findings of this study are available from the corresponding author upon reasonable request.

Keywords: 1,3-diaryltriazene · carbonic anhydrase · glaucoma · molecular docking · sulfaguanidine

[1] C. T. Supuran, *Nat. Rev. Drug Discovery* **2008**, *7*, 168–181.
[2] S. B. Ceyhun, M. Şentürk, E. Yerlikaya, O. Erdoğan, Ö. İ. Küfrevioğlu, D. Ekinci, *Environ. Toxicol. Pharmacol.* **2011**, *32*, 69–74.
[3] F. Carta, L. Di Cesare Mannelli, M. Pinard, C. Ghelardini, A. Scozzafava, R. McKenna, C. T. Supuran, *Bioorg. Med. Chem.* **2015**, *23*, 1828–1840.
[4] V. M. Krishnamurthy, G. K. Kaufman, A. R. Urbach, I. Gitlin, K. L. Gudiksen, D. B. Weibel, G. M. Whitesides, *Chem. Rev.* **2008**, *108*, 946–1051.
[5] S. Akocak, C. T. Supuran, *J. Enzyme Inhib. Med. Chem.* **2019**, *34*, 1652–1659.
[6] S. Akocak, Ö. Güzel-Akdemir, R. Kishore Kumar Sanku, S. S. Russom, B. I. Iorga, C. T. Supuran, M. A. Ilies, *Bioorg. Chem.* **2020**, *103*, 104204.
[7] J. T. Andring, M. Fouch, S. Akocak, A. Angeli, C. T. Supuran, M. A. Ilies, R. McKenna, *J. Med. Chem.* **2020**, *63*, 13064–13075.
[8] C. T. Supuran, A. Scozzafava, *Bioorg. Med. Chem.* **2007**, *15*, 4336–4350.
[9] M. Aggarwal, R. McKenna, *Expert Opin. Ther. Pat.* **2012**, *22*, 903–915.
[10] M. F. Sugrue, *Prog. Retinal Eye Res.* **2000**, *19*, 87–112.
[11] R. Ulus, M. Kaya, D. Demir, E. Tunca, M. Bülbül, *J. Enzyme Inhib. Med. Chem.* **2016**, *31*, 63–69.
[12] S. Akocak, P. Taslimi, N. Lolak, M. Işık, M. Durgun, Y. Budak, C. Türkeş, İ. Gülçin, Ş. Beydemir, *Chem. Biodiversity* **2021**, *18*, e2000958.
[13] M. Işık, Ş. Beydemir, *Arch. Physiol. Biochem.* **2022**, *128*, 352–359.
[14] C. Ward, S. P. Langdon, P. Mullen, A. L. Harris, D. J. Harrison, C. T. Supuran, I. H. Kunkler, *Cancer Treat. Rev.* **2013**, *39*, 171–179.
[15] C. B. Mishra, S. Kumari, A. Angeli, S. Bua, M. Tiwari, C. T. Supuran, *J. Med. Chem.* **2018**, *61*, 3151–3165.
[16] N. Lolak, S. Akocak, S. Bua, R. K. K. Sanku, C. T. Supuran, *Bioorg. Med. Chem.* **2019**, *27*, 1588–1594.
[17] C. T. Supuran, *Biochem. J.* **2016**, *473*, 2023–2032.
[18] C. Türkeş, S. Akocak, M. Işık, N. Lolak, P. Taslimi, M. Durgun, İ. Gülçin, Y. Budak, Ş. Beydemir, *J. Biomol. Struct. Dyn.* **2022**, *40*, 8752–8764.
[19] P. Taslimi, M. Işık, F. Türkan, M. Durgun, C. Türkeş, İ. Gülçin, Ş. Beydemir, *J. Biomol. Struct. Dyn.* **2021**, *39*, 5449–5460.
[20] Y. Lou, P. C. McDonald, A. Oloumi, S. Chia, C. Ostlund, A. Ahmadi, A. Kyle, U. auf dem Keller, S. Leung, D. Huntsman, B. Clarke, B. W. Sutherland, D. Waterhouse, M. Bally, C. Roskelley, C. M. Overall, A. Minchinton, F. Pacchiano, F. Carta, A. Scozzafava, N. Touisni, J.-Y. Winum, C. T. Supuran, S. Dedhar, *Cancer Res.* **2011**, *71*, 3364–3376.
[21] C. T. Supuran, *J. Enzyme Inhib. Med. Chem.* **2012**, *27*, 759–772.
[22] F. Mincione, M. Starnotti, L. Menabuoni, A. Scozzafava, A. Casini, C. T. Supuran, *Bioorg. Med. Chem. Lett.* **2001**, *11*, 1787–1791.
[23] Multifaceted clinical effects of acetazolamide: will the underlying mechanisms please stand up?.
[24] E. R. Swenson, *Expert Opin. Drug Saf.* **2014**, *13*, 459–472.
[25] P. Sharma, V. Dayma, A. Dwivedi, P. K. Baroliya, I. P. Tripathi, M. Vanangamudi, R. S. Chauhan, A. K. Goswami, *Bioorg. Chem.* **2020**, *96*, 103642.
[26] D. B. Kimball, M. M. Haley, *Angew. Chem. Int. Ed.* **2002**, *41*, 3338–3351.
[27] F. Marchesi, M. Turriziani, G. Tortorelli, G. Avvisati, F. Torino, L. De Vecchis, *Pharmacol. Res.* **2007**, *56*, 275–287.
[28] A. Sousa, F. Santos, M. M. Gaspar, S. Calado, J. D. Pereira, E. Mendes, A. P. Francisco, M. J. Perry, *Bioorg. Med. Chem.* **2017**, *25*, 3900–3910.
[29] H. Adibi, M. B. Majnooni, A. Mostafaie, K. Mansouri, M. Mohammadi, *Iranian J. Pharmaceutical Research: IJPR* **2013**, *12*, 695.
[30] D. Canakci, I. Koyuncu, N. Lolak, M. Durgun, S. Akocak, C. T. Supuran, *J. Enzyme Inhib. Med. Chem.* **2019**, *34*, 110–116.
[31] N. Lolak, S. Akocak, S. Bua, M. Koca, C. T. Supuran, *Bioorg. Chem.* **2018**, *77*, 542–547.
[32] S. Akocak, N. Lolak, S. Bua, C. T. Supuran, *J. Enzyme Inhib. Med. Chem.* **2018**, *33*, 1575–1580.
[33] SitaRam, G. Celik, P. Khloya, D. Vullo, C. T. Supuran, P. K. Sharma, *Bioorg. Med. Chem.* **2014**, *22*, 1873–1882.
[34] S. Göksu, A. Naderi, Y. Akbaba, P. Kalın, A. Akıncıoğlu, İ. Gülçin, S. Durdagi, R. E. Salmas, *Bioorg. Chem.* **2014**, *56*, 75–82.
[35] A. K. Saluja, M. Tiwari, D. Vullo, C. T. Supuran, *Bioorg. Med. Chem. Lett.* **2014**, *24*, 1310–1314.
[36] M. Bozdag, A. M. Alafeefy, F. Carta, M. Ceruso, A.-M. S. Al-Tamimi, A. A. Al-Kahtani, F. A. S. Alasmary, C. T. Supuran, *Bioorg. Med. Chem.* **2016**, *24*, 4100–4107.
[37] M. Işık, S. Akocak, N. Lolak, P. Taslimi, C. Türkeş, İ. Gülçin, M. Durgun, Ş. Beydemir, *Arch. Pharm. (Weinheim, Ger.)* **2020**, *353*, 2000102.
[38] Schrödinger Release 2022–3: QikProp, Schrödinger, LLC, New York, NY, 2022.
[39] C. A. Lipinski, F. Lombardo, B. W. Dominy, P. J. Feeney, *Adv. Drug Delivery Rev.* **1997**, *23*, 3–25.
[40] E. M. Duffy, W. L. Jorgensen, *J. Am. Chem. Soc.* **2000**, *122*, 2878–2888.
[41] M. Durgun, C. Türkeş, M. Işık, Y. Demir, A. Saklı, A. Kuru, A. Güzel, Ş. Beydemir, S. Akocak, S. M. Osman, Z. AlOthman, C. T. Supuran, *J. Enzyme Inhib. Med. Chem.* **2020**, *35*, 950–962.
[42] N. Lolak, S. Akocak, M. Durgun, H. E. Duran, A. Necip, C. Türkeş, M. Işık, Ş. Beydemir, *Mol. Diversity* **2022**.
[43] N. Lolak, S. Akocak, C. Türkeş, P. Taslimi, M. Işık, Ş. Beydemir, İ. Gülçin, M. Durgun, *Bioorg. Chem.* **2020**, *100*, 103897.
[44] J. A. Verpoorte, S. Mehta, J. T. Edsall, *J. Biol. Chem.* **1967**, *242*, 4221–4229.
[45] H. Yakan, H. Muğlu, C. Türkeş, Y. Demir, M. Erdoğan, M. S. Çavuş, Ş. Beydemir, *J. Mol. Struct.* **2023**, *1280*, 135077.
[46] H. Lineweaver, D. Burk, *J. Am. Chem. Soc.* **1934**, *56*, 658–666.
[47] M. Işık, Ş. Beydemir, *J. Biomol. Struct. Dyn.* **2021**, *39*, 6515–6523.
[48] S. Chakravarty, K. K. Kannan, *J. Mol. Biol.* **1994**, *243*, 298–309.
[49] Schrödinger Release 2022–3: Protein Preparation Wizard, Schrödinger, LLC, New York, NY, 2022.
[50] K. Yararli, E. B. Ozer, S. Bayindir, C. Caglayan, C. Turkes, S. Beydemir, *J. Mol. Struct.* **2023**, *1276*, 134783.
[51] G. Madhavi Sastry, M. Adzhigirey, T. Day, R. Annabhimoju, W. Sherman, *J. Comput.-Aided Mol. Des.* **2013**, *27*, 221–234.
[52] C. Kakakhan, C. Türkeş, Ö. Güleç, Y. Demir, M. Arslan, G. Özkemahlı, Ş. Beydemir, *Bioorg. Med. Chem.* **2023**, *77*, 117111.
[53] D. Osmaniye, C. Türkeş, Y. Demir, Y. Özkay, Ş. Beydemir, Z. A. Kaplancıklı, *Arch. Pharm. (Weinheim, Ger.)* **2022**, *355*, 2200132.
[54] Schrödinger Release 2022–3: LigPrep, Schrödinger, LLC, New York, NY, 2022.
[55] Ö. Güleç, C. Türkeş, M. Arslan, Y. Demir, Y. Yeni, A. Hacımüftüoğlu, E. Ereminsoy, Ö. İ. Küfrevioğlu, Ş. Beydemir, *Mol. Diversity* **2022**, *26*, 2825–2845.
[56] Schrödinger Release 2022–3: Receptor Grid Generation, Schrödinger, LLC, New York, NY, 2022.
[57] Schrödinger Release 2022–3: Glide, Schrödinger, LLC, New York, NY, 2022.
[58] R. A. Friesner, J. L. Banks, R. B. Murphy, T. A. Halgren, J. J. Klicic, D. T. Mainz, M. P. Repasky, E. H. Knoll, M. Shelley, J. K. Perry, D. E. Shaw, P. Francis, P. S. Shenkin, *J. Med. Chem.* **2004**, *47*, 1739–1749.
[59] R. A. Friesner, R. B. Murphy, M. P. Repasky, L. L. Frye, J. R. Greenwood, T. A. Halgren, P. C. Sanschagrin, D. T. Mainz, *J. Med. Chem.* **2006**, *49*, 6177–6196.
[60] Y. Demir, C. Türkeş, M. S. Çavuş, M. Erdoğan, H. Muğlu, H. Yakan, Ş. Beydemir, *Arch. Pharm. (Weinheim, Ger.)* **2022**, *356*, 2200554.
[61] Schrödinger Release 2022–3: Epik, Schrödinger, LLC, New York, NY, 2022.
[62] J. C. Shelley, A. Cholleti, L. L. Frye, J. R. Greenwood, M. R. Timlin, M. Uchimaya, *J. Comput.-Aided Mol. Des.* **2007**, *21*, 681–691.
[63] Schrödinger Release 2022–3: Prime, Schrödinger, LLC, New York, NY, 2022.
[64] G. Barreiro, C. R. W. Guimarães, I. Tubert-Brohman, T. M. Lyons, J. Tirado-Rives, W. L. Jorgensen, *J. Chem. Inf. Model.* **2007**, *47*, 2416–2428.
[65] S. A. Güngör, M. Köse, M. Tümer, C. Türkeş, Ş. Beydemir, *J. Biomol. Struct. Dyn.* **2022**, 1–11.
[66] Schrödinger Release 2022–3: Maestro, Schrödinger, LLC, New York, NY, 2022.
[67] A. Buza, C. Türkeş, M. Arslan, Y. Demir, B. Dincer, A. R. Nixha, Ş. Beydemir, *Int. J. Biol. Macromol.* **2023**, *239*, 124232.

Manuscript received: April 29, 2023
Accepted manuscript online: July 20, 2023
Version of record online: August 4, 2023